Advances in Cancer Biology - Metastasis 17 (2026) 100184

Contents lists available at ScienceDirect

Advances in Cancer Biology - Metastasis

journal homepage: www.journals.elsevier.com/advances-in-cancer-biology-metastasis

Chronic insulin exposure induces EMT-associated changes and increases migration and invasion in cancer cells

Jaume Margalef Rieres [a], Patricia González-Sáenz [b], Sylvain Ladame [a,1,*], Nuria Oliva [a,b,1,**]

[a] Department of Bioengineering, Imperial College London, White City Campus, London, W12 0BZ, UK
[b] Department of Bioengineering, Institut Quimic de Sarria, Via Augusta 390, 08017, Barcelona, Spain

ARTICLE INFO

Keywords:
Insulin
EMT
TME
SKOV3
Migration
Invasion
Hyperinsulinemia

ABSTRACT

Metastasis significantly worsens cancer prognosis and survival, and epidemiological studies suggest that metabolic disorders such as Type 2 Diabetes Mellitus (T2DM) may be associated with poorer cancer outcomes. Recent studies emphasize changes in the tumor microenvironment (TME), including angiogenesis and epithelial-to-mesenchymal transition (EMT); however, early detection of metastasis and identification of high-risk TME factors remain challenging. Because insulin is elevated in hyperinsulinemic states and can influence growth-related signalling pathways, we investigated whether chronic insulin exposure promotes EMT-associated and invasion-associated changes using SKOV3 ovarian cancer cells as an *in vitro* model. Insulin exposure was associated with altered expression of EMT-related genes, changes in epithelial and mesenchymal markers, and increased migration and invasion *in vitro*. Supportive RT-qPCR analyzes in A549 and MDA-MB-231 cells showed similar insulin-associated changes in selected transcriptional markers, providing valuable insights into the role of insulin in cancer metastasis, potentially opening an avenue for further exploration of the connection between T2DM and metastatic progression in a broader range of tumors and *in vivo* models.

1. Introduction

Cancer accounts for nearly one in six deaths worldwide, with approximately 80% of those diagnosed with metastatic cancer ultimately succumbing to the disease [1]. It has been previously demonstrated that insulin plays a key role in cancer incidence and progression. Indeed, overweight and obese individuals, whose lifetime insulin production can triple compared to that of healthy individuals, face an increased risk of developing cancer, with a global study revealing that excess body weight accounted for approximately 3.9% of all cancer cases in 2012 (544,300 cases) [2]. In addition, the role of insulin in Type 2 Diabetes Mellitus (T2DM) has been linked to the progression of oral squamous cell carcinoma [3]. Furthermore, individuals with T2DM appear more susceptible to high metastatic involvement [4]. For instance, Baleiras et al. identified T2DM as a negative prognostic factor for survival in metastatic colorectal cancer (mCRC) [5]. These observations prompt a key question: given that insulin is the primary hormone upregulated in T2DM, and that it is also a risk factor for cancer in general, could it also be instrumental in triggering metastasis? Such a correlation and its underlying mechanism have not yet been described in

Abbreviations: AKT, Protein kinase B; ANOVA, Analysis of Variance; AU, Fluorescence Arbitrary Units; BSA, Bovine serum albumin; BCA, bicinchoninic acid; CO_2, Carbon dioxide; cDNA, Complementary Deoxyribonucleic acid; DMEM, Dulbecco's Modified Eagle Medium; DAPI, 4′,6-diamidino-2-phenylindole; ECM, Extracellular matrix; EMT, Epithelial-to-Mesenchymal Transition; FBS, Foetal bovine serum; ERK, Extracellular Signal-Regulated Kinase; GAPDH, Glyceraldehyde-3-phosphate dehydrogenase; HRP, Horseradish Peroxidase; I50, Insulin 50 μg/ml concentration; ICC, Immunocytochemistry; IGF-1, Insulin Growth Factor 1; IGF-1R, Insulin Growth Factor Receptor 1; IRS, Insulin Receptor Substrate; MAPK, Mitogen-activated protein kinase; MMPs, Matrix metalloproteinases; MTT, 3-(4,5-dimethylthiazol-2-yl)-2,5-diphenyltetrazolium bromide; NGS, Normal Goat Serum; O.D., Optical Density; PBS, Phosphate-buffered saline; PBST, Phosphate-buffered saline +0.1% Tween 20; PI3K, Phosphoinositide 3-kinase; p-IRS, Phosphorylated Insulin Receptor Substrate; PVDF, Polyvinylidene difluoride; RIPA, Radioimmunoprecipitation assay; RNA, Ribonucleic acid; RT, Reverse transcriptase; RT-qPCR, Reverse transcription-quantitative polymerase chain reaction; SEM, Standard Error of the Mean; SMADs, Mothers against decapentaplegic homolog; SNAI1, Snail Family Transcriptional Repressor 1; T2DM, Type 2 Diabetes Mellitus; TGF-β, Transforming growth factor beta; TME, Tumor microenvironment; ZO-1, Zonula occludens-1.

* Corresponding author.
** Corresponding author.
E-mail addresses: s.ladame@imperial.ac.uk (S. Ladame), nuria.oliva@iqs.url.edu (N. Oliva).
[1] Equal contribution.

https://doi.org/10.1016/j.adcanc.2026.100184
Received 17 October 2025; Received in revised form 13 April 2026; Accepted 13 April 2026
Available online 16 April 2026

the literature. These observations raise the possibility that insulin may contribute to cellular programs associated with metastatic progression. In this study, we examined whether chronic insulin exposure promotes EMT-associated gene expression and *in vitro* migratory and invasive behavior, focusing primarily on SKOV3 ovarian cancer cells and including supportive RT-qPCR analyzes in A549 and MDA-MB-231 cells.

The mechanisms behind metastasis remain poorly understood [6]. A key concept that has recently come to the forefront of discussions is the influence of endocrinological regulation on the tumor microenvironment (TME) and its role in driving metastatic potential [7,8]. Understanding how metabolic changes within the TME enable cancer cells to acquire invasive traits could offer crucial insights into triggers of metastasis and lead to more personalized cancer treatments [9]. Additionally, this link between signalling molecules, such as insulin, and observable phenotypic effects may further clarify the pathways leading to metastatic progression.

Recent advancements in sequencing and lineage tracing have underscored the heterogeneity of tumor progression, emphasizing the importance of epithelial-to-mesenchymal transition (EMT) in metastasis initiation [10]. EMT, a process where epithelial cells adopt a mesenchymal phenotype [11] is driven by factors such as MMPs and growth signals, enabling cells to invade and resist stress [12]. In breast cancer, MMP-9 is particularly significant in the early stages of tumorigenesis, thus contributing to the formation of the metastatic niche [13]. One key observation in EMT is the direct repression of E-cadherin by the transcription factor SNAI1 [14]. Transcription factors play a crucial role in driving the transition by suppressing epithelial genes and activating mesenchymal genes [15]. For instance, the stimulation of mouse hepatocytes with TGF-β induces EMT and enhances cell intravasation [16].

While insulin is best known for regulating glucose uptake [17], it also plays a significant role in cellular growth and proliferation [18]. In hyperinsulinemic conditions, insulin's mitogenic effects extend beyond normal pathways, activating both PI3K/AKT and MAPK signalling and potentially promoting cancer cell invasion through EMT [19,20]. Could this vital hormone help explain the lower survival rates and increased metastatic risk observed in diabetic cancer patients? Recent research highlights the role of insulin as a key proliferative agent in cancer biology [21–23]. Notably, individuals who maintain normal blood glucose levels but exhibit persistent hyperinsulinemia may still be at increased risk of cancer. Elevated circulating insulin has been associated with tumor growth and cancer mortality independent of diabetes in several studies [24]. This may contribute to carcinogenesis through activation of mitogenic signalling pathways and increased insulin-like growth factor-1 (IGF-1) activity that promote tumor growth and progression [24–27]. We hypothesize that, beyond driving cell proliferation, insulin may also induce phenotypic changes in non-metastatic SKOV3 cells via the EMT cascade, thereby facilitating invasive behavior (Fig. 1). This was investigated through assessment of EMT-associated gene expression (RT-qPCR), phenotypic markers (ICC), functional migration and invasion assays, and western blotting to probe insulin-responsive signalling pathway activation.

In this study, we show that chronic insulin exposure is associated with EMT-like marker changes in SKOV3 cells, together with increased migration and invasion *in vitro*. Additional RT-qPCR analyzes in A549 and MDA-MB-231 cells showed similar changes in selected transcriptional markers; however, the functional, protein-level, and signalling conclusions remain centered on the SKOV3 model.

2. Materials and methods

2.1. Tissue culture reagents and materials

SKOV3 human non-metastatic ovarian adenocarcinoma cells with an epithelial-like morphology and resistance to tumor necrosis factors were cultured in DMEM supplemented with 10% FBS, 1% penicillin/streptomycin, and 10% L-glutamate (Thermo Fisher Scientific, Inc.). For experimental conditions, media was also supplemented with 2 μg/mL, 4 μg/mL, or 8 μg/mL of human insulin (Thermo Fisher Scientific, Inc.) to simulate lower-dose chronic *in vitro* exposure conditions, or 50 μg/mL to model a high-dose chronic insulin exposure condition. Media were

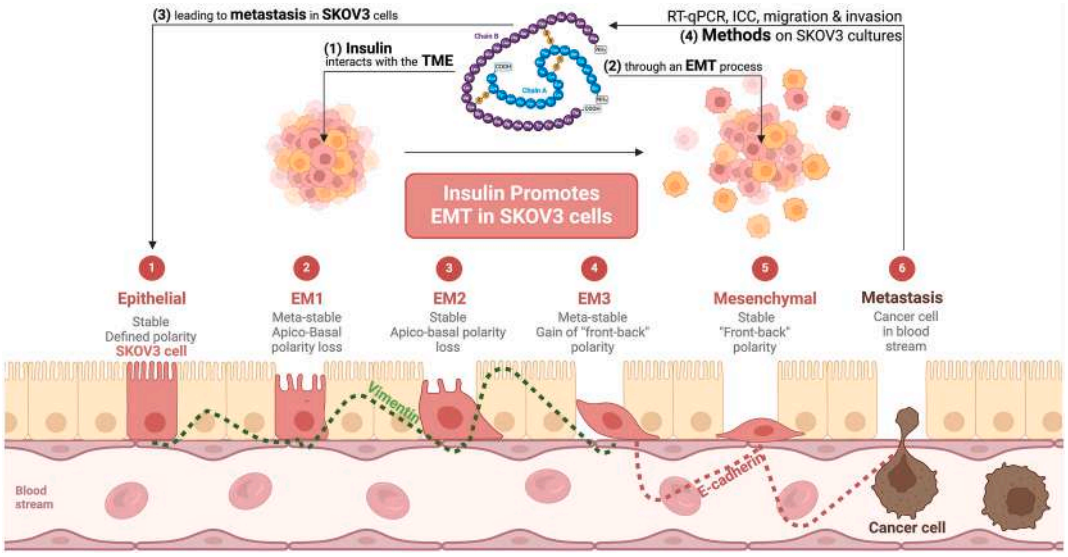

Fig. 1. Graphical abstract illustrating a proposed model by which chronic insulin exposure may promote EMT-associated changes and increased migration/invasion *in vitro*. Insulin interaction with the tumor microenvironment (TME) is hypothesized, based on existing literature, to influence signalling pathways such as RAS/MAPK and PI3K/Akt [15,18,19]. Downstream gene expression changes associated with EMT were assessed using RT-qPCR, including effectors such as TGF-β, SMAD proteins, and matrix metalloproteinase-9 (MMP-9). EMT-related phenotypic features were evaluated using immunocytochemistry (ICC) and functional migration and invasion assays. These analyzes demonstrated changes consistent with EMT progression, including downregulation of E-cadherin, upregulation of vimentin, loss of apico-basal polarity, and acquisition of a more motile, mesenchymal phenotype. Progression through intermediate EMT states (EM1-EM3) is shown as literature-based context for how EMT-associated phenotypes can support motility and invasiveness; metastatic dissemination itself was not directly assessed in the present study.

changed every 2-3 days, and cells passaged when they reached 80-90% confluence. At 7, 14, 21, and 28 days, metastatic behavior was assessed as described below.

2.2. Cell viability assay

To evaluate cell viability after incubation at different time points (7, 14, 21, and 28 days) with varying insulin concentrations (control without insulin, 2 μg/mL, 4 μg/mL, 8 μg/mL, and 50 μg/mL), the 3-(4,5-dimethylthiazol-2-yl)-2,5-diphenyltetrazolium bromide (MTT) assay was used. Cells cultured in 96-well plates were subjected to the indicated experimental conditions and times at 37 °C and 5% CO_2. Subsequently, they were washed with PBS and incubated in complete medium supplemented with MTT solution (0.5 mg/mL), added at 10% v/v, for 3 h at 37 °C and 5% CO_2. DMSO was then added to solubilize the formazan crystals formed. The absorbance at 550 nm was then measured using a plate reader (Infinite® 200 PRO, Tecan Life Sciences), and values were expressed as percentages of cell viability relative to untreated cells by normalizing to their absorbance.

2.3. Gene expression analysis

Total RNA from SKOV3 ovarian cancer cells was extracted using RNeasy Plus Mini kit (Qiagen, Inc.) and converted to cDNA using SuperScript™ IV Reverse Transcriptase (RT) enzyme (Invitrogen; Thermo Fisher Scientific, Inc.) following manufacturer's protocol. For RT-qPCR analysis, SYBR™ Green PCR Master Mix (Applied Biosystems) was used with primers specific to our target genes, in accordance with the manufacturer's protocol. Primers were designed against the UCSC Genome Browser (GAPDH **Fw**: GTCTCCTCTGACTTCAACAGCG, **Rv**: ACCACCCTGTTGCTGTAGCCAA; MMP9 **Fw**: GCCACTACTGTGCCTTTGAGTC, **Rv**: CCCTCAGAGAATCGCCAGTACT; TGF-B **Fw**: TACCTGAACCCGTGTTGCTCTC, **Rv**: GTTGCTGAGGTATCGCCAGGAA; SMAD3 **Fw**: TGAGGCTGTCTACCAGTTGACC, **Rv**: GTGAGGACCTTGTCAAGCCACT).

Gene expression was determined as a fold change after normalizing to the housekeeping gene GAPDH, using the $2^{-\Delta\Delta Ct}$ method. Statistical comparisons between two groups were performed using an unpaired Student's t-test in Prism v9.2. A p-value of less than 0.05 was considered statistically significant. Each experimental condition and target gene were tested in triplicate (n = 3 biological replicates), with three technical replicates taken from each biological replicate (n = 9).

To assess whether the insulin-associated transcriptional response extended beyond SKOV3 cells, additional RT-qPCR analyzes of MMP-9 and TGF-β were performed in the lung cancer cell line A549 and the metastatic breast cancer cell line MDA-MB-231 (Supplementary Figs. 1 and 2).

2.4. Protein expression analysis

After insulin treatments (2 μg/mL; 4 μg/mL; 8 μg/mL and 50 μg/mL) at different time points (7, 14, 21 and 28 days), cells were washed with PBS, scrapped and lyzed using cold RIPA buffer (200 mM Tris–HCl at pH: 7.4, 130 mM sodium chloride, 10% glycerol, 0.1% SDS, 1%Triton X-100 and 10 mM magnesium chloride) supplemented with protease and phosphatase inhibitors (Sigma-Aldrich). Then, lysates were centrifuged (30 min, 18,000*g*, 4 °C). From those tubes, total protein lysates were quantified using a BCA protein quantification kit (Pierce™ BCA Protein Assay Kits, Thermo Scientific), subjected to electrophoresis, and subsequently electrotransferred onto a PVDF membrane. Those membranes were then incubated in 5% BSA blocking buffer for 1 h at room temperature and then probed with the following antibodies: p-IGF1R/p-IR (dilution 1:1000, 44-804G, Thermo Fisher), p-IRS (dilution 1:1000, 44-816F, Thermo Fisher), pAKT (dilution 1:1000, 649001, BioLegend) and pERK (dilution 1:1000, 14-9109-82, Thermo Fisher) at 4 °C overnight. Protein levels were normalized with GAPDH (dilution 1:50000, MA5-35235, Thermo Fisher). Detection of proteins was performed using horseradish-peroxidase-conjugated secondary antibodies. Specific antigen–antibody binding was visualized with chemiluminescence method according to the manufacturer's instructions (HRP substrate for immunotransference, Western Immobilon Forte, Millipore) using the Amersham™ ImageQuant™ 800 Western blot imaging system.

2.5. Invasion and migration assays

For the migration assay, 100,000 cells in serum-free cell culture media were seeded on top of a Transwell® filter membrane with 8 μm pores (Corning), and 600 μl of cell media containing FBS as a chemoattractant were added to the lower chamber of a 24-well plate, ensuring contact with the membrane in the upper well to create a chemoattractant gradient for cell motility. The cells were then incubated for 24 h at 37 °C and 5% CO_2. For the invasion assay, the same procedure was followed, with the addition of 100 μl of Corning® Matrigel® Matrix (Corning) on top of the Transwell® membrane prior to adding the cell solution, following the manufacturer's protocol. After the 24-h incubation period, the media and non-migrated cells were removed from the top of the Transwell® membrane using a cotton-tipped applicator. The Transwell® insert was then submerged into a well containing 600-1000 μl of 70% ethanol for 10 min. Excess ethanol was washed from the top of the membrane, and the membrane was submerged in a 0.2% crystal violet solution (Abcam) for 5-10 min at room temperature, submerged into 600-1000 μl of solubilisation solution, and the optical density (O.D.) was read using a CLARIOstar Plus plate reader at a wavelength of 595 nm.

2.6. Immunocytochemistry

Immunocytochemistry was performed using the following primary antibodies: CD323 anti-E-cadherin (AB-1210458, anti-rat, monoclonal, 1:100), anti-Vimentin (AB-2216267, anti-chicken, polyclonal, 1:1000), and ZO1-1A12 (AB-2533147), anti-mouse, monoclonal, 1:100), p-IRS (44-816F, anti-rabbit, 1:100). The associated secondary antibodies were as follows: Goat anti-Chicken IgY (H + L), Alexa Fluor™ 647 (AB-2535866, polyclonal, 1:1000), Goat anti-Rat IgG (H + L) Cross-Adsorbed Antibody, Alexa Fluor™ 488 (AB-2534074, polyclonal, 1:100), Goat anti-Mouse IgG (H + L) Cross-Adsorbed Antibody, Alexa Fluor™ 647 (AB-2535804, polyclonal, 1:100), Goat anti-rabbit IgG (H + L) Alexa Fluor ™ 568 (A-11011, polyclonal, 1:1000, Thermo Fisher). Alexa Fluor™ 488 Phalloidin and DAPI were used as a counterstaining. Cells grown on gelatine-coated glass coverslips were fixed in 4% paraformaldehyde (in case of permeabilization of the cells, 0.02% of Triton X-100 in PBS was added) at pH 7.4 for 10 min at room temperature. To block nonspecific antibody binding, the cells were then incubated with a solution of 5% Normal Goat Serum (NGS), 3% Bovine Serum Albumin (BSA), and 22.52 mg/mL glycine in PBST (PBS + 0.1% Tween 20) for 30 min. Subsequently, the cells were incubated with the diluted primary antibody in 5% NGS and 1% BSA in PBST for 1 h at room temperature, inside a humidified chamber. After incubation, the cells were washed three times with PBS for 5 min each, followed by incubation with the appropriate secondary antibody solution (diluted in 5% NGS and 1% BSA in PBST) for 1 h at room temperature in the dark. Then, cells were washed three times with PBS for 5 min each and mounted using Fluoromount-G™ Mounting Medium containing DAPI. All the reagents used in the procedure were purchased from Thermo Fisher Scientific, Inc. Image analysis and pixel intensity quantification was done using ImageJ. Fluorescence intensity measurements were obtained from pixels expressing fluorescence, excluding nuclear emission to avoid crosstalk between DAPI fluorescence and the AlexaFluor fluorophores. A threshold limit was applied for fluorescence detection, and mean values were plotted.

2.7. Statistical testing and data analysis

All experiments were carried out in triplicates. For statistical analysis between two samples, an unpaired *t*-test was employed to compare the control and experimental groups. When comparing multiple groups, a one-way ANOVA test was utilized, followed by a Dunnett's post hoc test. A significance threshold of $p < .05$ was considered statistically significant. The data are presented as mean ± standard error of the mean using

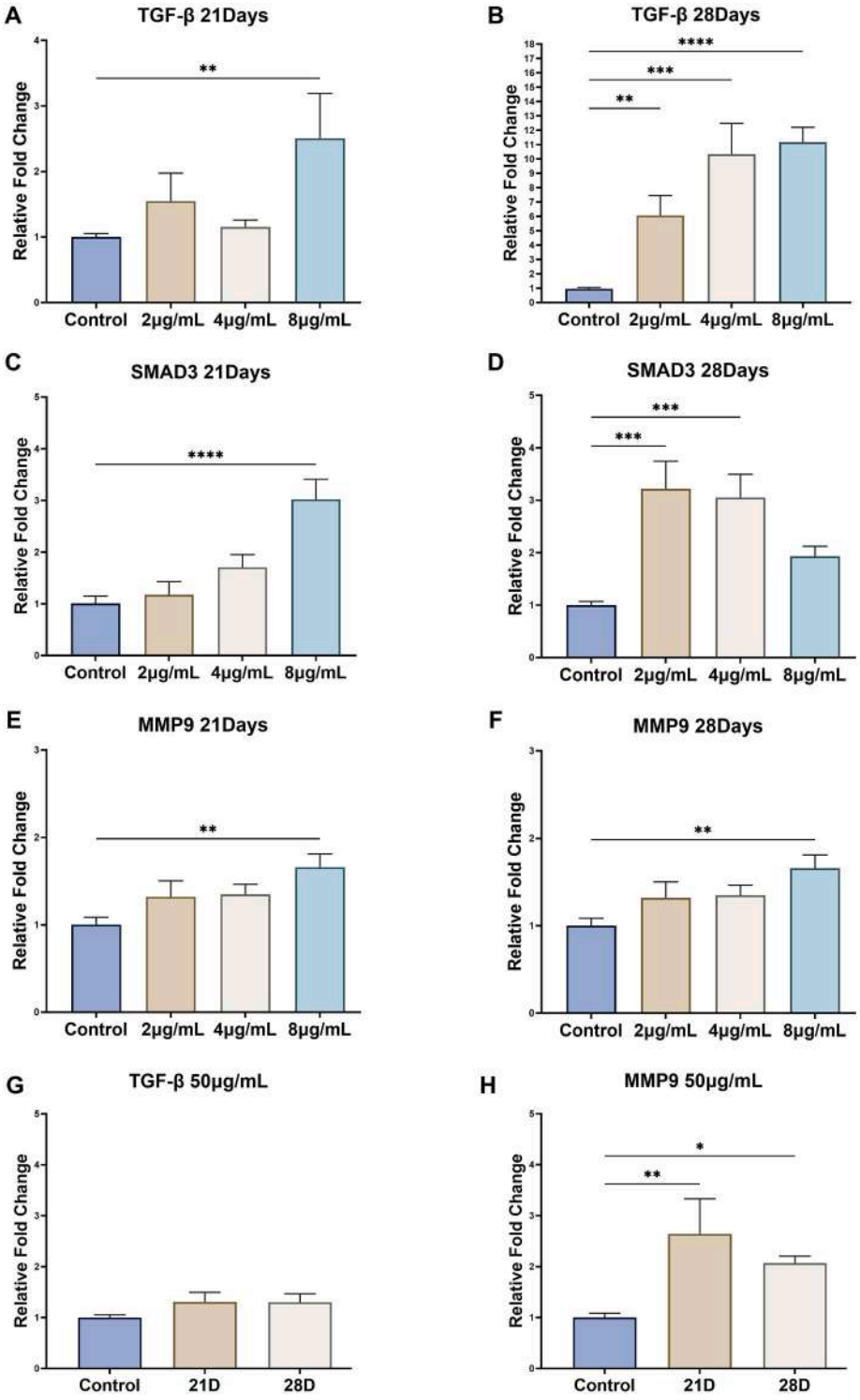

Fig. 2. Dose- and time-dependent effects of insulin on TGF-β, SMAD3, and MMP-9 expression in SKOV3 cells. Effects of Insulin on the Relative Gene Expression of (A-B, G) TGF-β, (C-D) SMAD3, and (E-F, H) MMP-9 in SKOV3 Cells after 21 and 28 Days of Culture under Various Insulin Concentrations. Relative gene expression was analyzed in SKOV3 cells cultured with 2, 4, 8, and 50 µg/mL insulin for 21 or 28 days. Earlier time points (7 and 14 days) did not demonstrate statistically significant changes and are therefore presented in the supplementary data. Each sample was labeled according to its corresponding insulin concentration, with the 50 µg/mL samples further categorized by exposure duration. RT-qPCR was used to quantify gene expression relative to GAPDH, the housekeeping gene. Expression levels were determined using the crossing point (CP) in PCR amplification, where sample fluorescence surpassed background levels. Data represent the mean ± SEM ($n = 3$). Statistical significance was assessed with thresholds of $P \leq .05$ (*), $P \leq .01$ (**), $P \leq .001$(***) and $P \leq .0001$ (****). Non-significant comparisons are not shown.

Prism v9.2 software. We assumed that both groups followed a Gaussian distribution and had equal variances, which were confirmed by verifying that variances were less than one in all three replicates for each experimental condition and by obtaining a negative result from an F-test.

3. Results

3.1. Insulin induces expression of EMT-associated factors in SKOV3 cells

The effect of insulin on the expression of TGF-β, SMAD3 and MMP-9 was first investigated over 28 days. Because prolonged exposure to high insulin concentrations could potentially affect cell survival, cell viability was also assessed under all experimental conditions. SKOV3 cells maintained high viability throughout the study (Supplementary Fig. 3), indicating that the observed transcriptional changes were not simply attributable to loss of cell viability.

Although the insulin concentrations used here exceed circulating human plasma levels, they were selected as chronic *in vitro* exposure conditions rather than as direct quantitative equivalents of clinical hyperinsulinemia. Insulin in the μg/mL range is commonly used in reduced-serum cell culture; for example, 1X ITS supplementation provides 10 μg/mL insulin, and several *in vitro* protocols use 5-10 μg/mL [28–30]. Higher nominal concentrations are often used *in vitro* because adsorption to culture materials reduces bioavailable insulin [31], and because static reduced-serum culture does not reproduce the spatial and temporal delivery of insulin *in vivo* [32,33]. Accordingly, the 50 μg/mL condition should be interpreted as an exploratory high-dose exposure used to assess dose-dependent responses under chronic culture conditions.

A concentration-related increase in expression levels of TGF-β was observed, and it became more pronounced with increasing incubation times at 21, and 28 days (Fig. 2A and B). For instance, after 21 days, a concentration of 8 μg/mL resulted in a 2.50-fold change ($P \leq .01$), which increased to 11.17-fold after 28 days ($P \leq .0001$). Similar patterns were observed for cells grown with insulin concentrations of 2 μg/mL and 4 μg/mL for 28 days (Fig. 2B), with maximum fold changes of 6.05 ($P \leq .01$) and 11.27 ($P \leq .001$), respectively. In contrast, the use of insulin at a concentration of 50 μg/mL resulted in decreased TGF-β levels, approaching control levels after both 21 and 28 days of culture (Fig. 2G).

Changes in SMAD3 expression exhibited a pattern similar to that of TGF-β between 21 days and 28 days (Fig. 2C and D). At an insulin concentration of 8 μg/mL, a significant 3.02-fold increase in expression was observed at 21 days ($P \leq .0001$). This decreased to 1.93-fold after 28 days (Fig. 2D), whereas TGF-β showed an 11.17-fold increase ($P \leq .0001$, Fig. 2B) and MMP-9 began to rise to 1.73-fold ($P \leq .01$, Fig. 2F). At lower insulin concentrations of 2 μg/mL and 4 μg/mL, the relative fold change in expression continued to increase with incubation time, reaching maxima of 3.22 ($P \leq .001$) and 3.05 ($P \leq .001$) after 28 days (Fig. 2D), respectively.

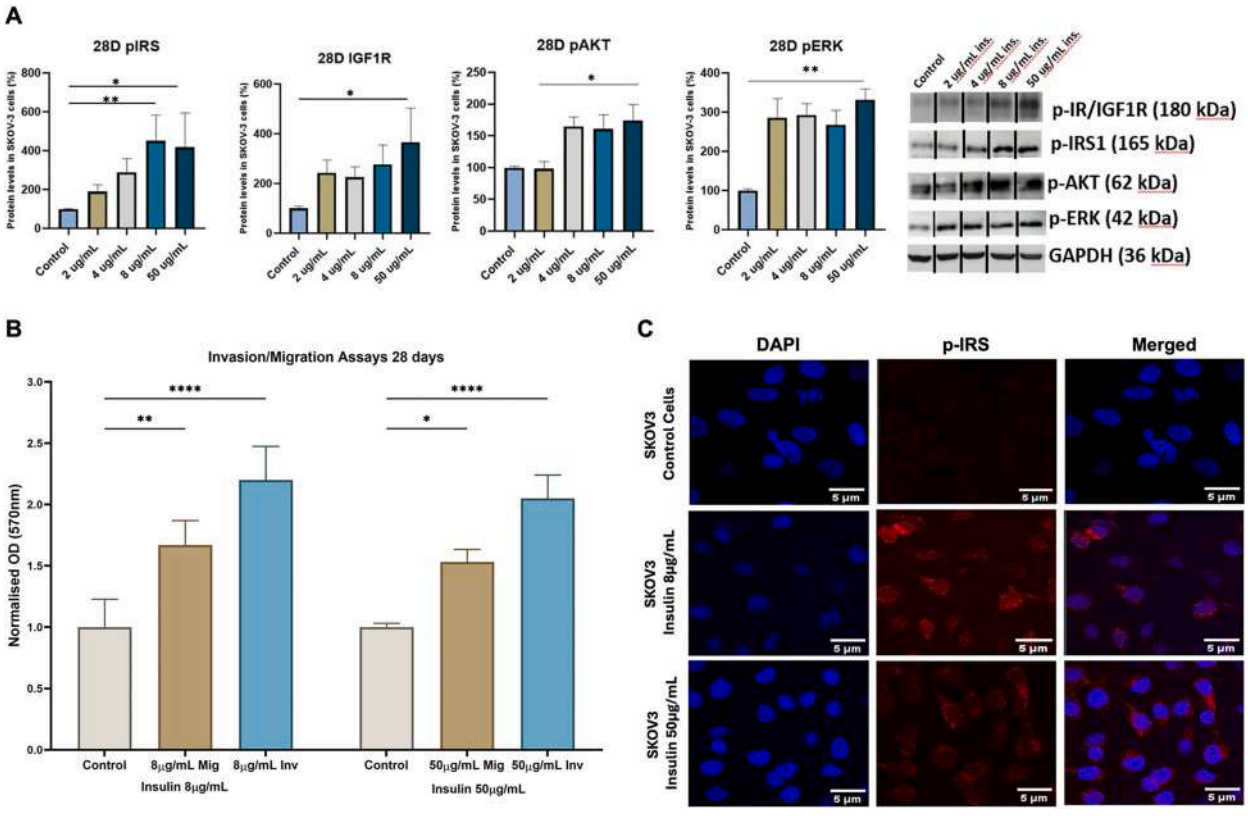

Fig. 3. Western blot analysis of insulin-responsive signalling and functional effects on migration and invasion in SKOV3 cells. A. Western blot analysis of total and phosphorylated proteins involved in insulin signalling pathways, including p-IRS, p-IR/IGF-1R, p-AKT, and p-ERK, in SKOV3 cells cultured with increasing insulin concentrations (2, 4, 8, and 50 μg/mL) at 28 days. Protein expression levels were normalized to GAPDH and quantified based on chemiluminescence intensity above background. Each lane corresponds to the indicated insulin concentration and time point. **B.** Effects of insulin on the migration and invasion capability of SKOV3 cells. Each sample was labeled based on the corresponding insulin concentration. The left panel shows the effects of 8 μg/mL insulin on cell migration and invasion after 28 days, while the right panel depicts the results for 50 μg/mL insulin. All quantitative data for both experiments are presented as mean ± SEM (n = 3) for all experiments. Statistical significance was defined as $P \leq .05$ (*), $P \leq .01$ (**), $P \leq .001$ (***) and $P \leq .0001$ (****). **C.** Phosphorylated IRS (p-IRS; red) levels in control (top row) and insulin-treated (bottom rows) SKOV3 cells. Nuclear DNA was stained with DAPI (blue). Qualitatively, p-IRS expression increased in insulin-treated cells compared to controls, with a greater increase observed at 50 μg/mL than at 8 μg/mL, although elevated expression was already evident at 8 μg/mL relative to control. Control and insulin-treated SKOV3 cells (8 and 50 μg/mL) were cultured for 28 days in the media described in Section 2.5 of the Methods.

A significant increase in MMP-9 expression was observed when SKOV3 cells were cultured with 8 μg/mL of insulin after 21 and 28 days ($P \leq .01$, Fig. 2E and F, respectively), and when the higher insulin concentration of 50 μg/mL was used at 21 days ($P \leq .01$) and 28 days ($P \leq .05$, Fig. 2H). For all three genes (TGF-β, SMAD3 and MMP-9), no significant changes in gene expression were observed at earlier time points (Supplementary Fig. 4).

Similar insulin-associated increases in MMP-9 and TGF-β gene expression were also observed in A549 lung cancer cells and MDA-MB-231 breast cancer cells (Supplementary Figs. 1 and 2), suggesting that this transcriptional response to chronic hyperinsulinemia is not restricted to SKOV3 cells and may reflect a broader metastasis-associated program.

3.2. Insulin induces time- and concentration-dependent activation of insulin/IGF-1R signalling pathways in SKOV3 cells

Western blot analysis (Fig. 3A and Supplementary Fig. 5) was performed to evaluate activation of insulin/IGF-1R-associated signalling pathways, and their link to genes related to proliferation, migration and differentiation, like pAKT and pERK. Protein levels were normalized to GAPDH and expressed relative to control.

Phosphorylation of IRS (p-IRS), an early mediator of insulin receptor signalling, was significantly increased at higher insulin concentrations (8 and 50 μg/mL), with delayed activation observed from day 14 onwards. Peak levels reached approximately 400–500-fold increases ($P \leq .05$–0.01), followed by partial reduction and stabilisation at later time points. Lower insulin concentrations did not induce significant changes. These findings were consistent with immunofluorescence data (Fig. 3C), which demonstrated greater p-IRS expression in cells treated with 50 μg/mL insulin compared to 8 μg/mL, although both conditions maintained elevated expression at 28 days. A similar trend was observed across other concentrations and time points (Supplementary Figs. 6 and 7).

In contrast, phosphorylated IGF-1R/IR (p-IGF-1R/p-IR) showed earlier activation, with significant increases detected at day 7 for both 8 and 50 μg/mL (~500–600-fold; $P \leq .05$–0.01). Expression remained elevated at 14 and 21 days before declining at day 28, where significance was retained only at 50 μg/mL.

Downstream signalling components demonstrated differential activation patterns. Phosphorylated AKT (pAKT) showed transient early activation at day 7 for higher concentrations, with levels returning to near baseline before a modest increase at day 28 (150–200-fold; $P \leq .05$). Conversely, phosphorylated ERK (pERK) exhibited delayed activation, with significant increases observed at day 21 (~500-fold; $P \leq .05$) for 8 and 50 μg/mL, and sustained activation at day 28 only in the highest concentration group (~350-fold; $P \leq .01$).

Overall, these results show concentration- and time-dependent changes in insulin-responsive signalling markers in SKOV3 cells. These changes paralleled the upregulation of EMT-related genes, supporting an association between chronic insulin exposure and pathway activation. However, because pathway inhibition and receptor-specific validation were not performed, these data should be interpreted as correlative rather than as proof that the observed EMT-associated changes are mediated through a specific signalling route.

3.3. Insulin enhances migration and invasion of SKOV3 cells

Metastatic activity of cells was next assessed through cell migration and invasion assays (Fig. 3B). Analysing migration and invasion activity is critical for assessing cancer progression, as higher levels of migratory and invasive activity correlate positively with increased inflammation and MMPs activity, which enable cells to intravasate more effectively. O.D. measurements were normalized by dividing each value by the mean of the corresponding control population.

The invasion capacity increased significantly 2.20-fold ($P \leq .001$) and 2.05-fold ($P \leq .0001$) when cells were exposed to 8 μg/mL and 50 μg/mL of insulin, respectively. Migration capacity also increased 1.67-fold ($P \leq .05$) with 8 μg/mL and 1.43-fold ($P \leq .01$) with 50 μg/mL. O.D. was analyzed at 28 days, as this time point coincided with the most significant genetic changes observed in the cell clusters.

3.4. Chronic insulin exposure is associated with EMT-like protein marker changes

To determine whether the observed genetic changes and migratory behavior were associated with proteomic alterations indicative of EMT, immunocytochemistry (ICC) analysis was performed to assess the expression of the epithelial markers E-cadherin [34] and ZO-1 [35], alongside the mesenchymal marker vimentin [36] (Fig. 4A–B).

Quantitative intensity analysis showed that E-cadherin levels decreased significantly from a mean value of 47.72 to 17.10 fluorescence arbitrary units (AU) ($P \leq .0001$, Fig. 4C) in SKOV3 cells cultured with insulin compared to the control cells. In contrast, vimentin expression increased from 69.56 to 104.36 AU ($P \leq .0001$, Fig. 4D), while ZO-1 levels decreased from 45.08 to 19.44 AU ($P \leq .0001$, Fig. 4E). These changes are consistent with an EMT-like shift in epithelial and mesenchymal marker expression, although additional protein-level validation and assessment of EMT transcription factors would be required to fully define the EMT program.

4. Discussion

This study contributes to the ongoing discussion on insulin's role in ovarian cancer biology, particularly its association with EMT-related molecular changes and increased migration and invasion in SKOV3 cells *in vitro*. Our findings demonstrate a clear association between elevated insulin concentrations and both transcriptional and phenotypic alterations in SKOV3 cells. Moreover, these results build on clinical observations in diabetic and overweight individuals, who exhibit hyperinsulinemia, further supporting a potential link between metabolic dysregulation and cancer progression. Previous studies support the broader relevance of hyperinsulinemia to cancer progression, although direct evidence specifically linking it to metastatic mechanisms remains limited and context dependent. Clinical data have associated hyperinsulinemia with increased cancer mortality and poorer outcomes, even outside overt diabetes [37,38], while experimental studies have shown that insulin can enhance proliferation, migration, and metastasis-related behavior in cancer cells *in vitro* [39]. In particular, insulin has been reported to increase motility and matrix metalloproteinase expression in colorectal cancer cells, supporting the concept that sustained insulin exposure may contribute to a pro-metastatic phenotype. Our findings are consistent with this broader framework and further suggest that chronic insulin exposure may promote metastasis-associated transcriptional and phenotypic changes in ovarian cancer cells.

We observed that higher insulin levels and prolonged exposure increased TGF-β, SMAD3, and MMP-9 expression, although the timing and magnitude of these responses varied (Fig. 2). We acknowledge that the delayed response likely reflects slow phenotypic adaptation under sustained exposure conditions, and that defining the precise basis of this timing is beyond the scope of the present study. Notably, insulin exposure was associated with EMT-related changes and increased migration and invasion *in vitro*, which are cellular traits relevant to metastatic progression. Importantly, supportive RT-qPCR experiments in A549 and MDA-MB-231 cells showed a similar trend toward insulin-associated MMP-9 upregulation (Supplementary Figs. 1 and 2, respectively), suggesting that this response may not be restricted to a single cell line.

TGF-beta has context-dependent roles in tumorigenesis, including reported effects on EMT and invasion-related programs [40]. In the present study, chronic insulin exposure was associated with changes in TGF-beta, SMAD3, and MMP-9 expression, although the timing and magnitude of these responses differed. Importantly, our data do not

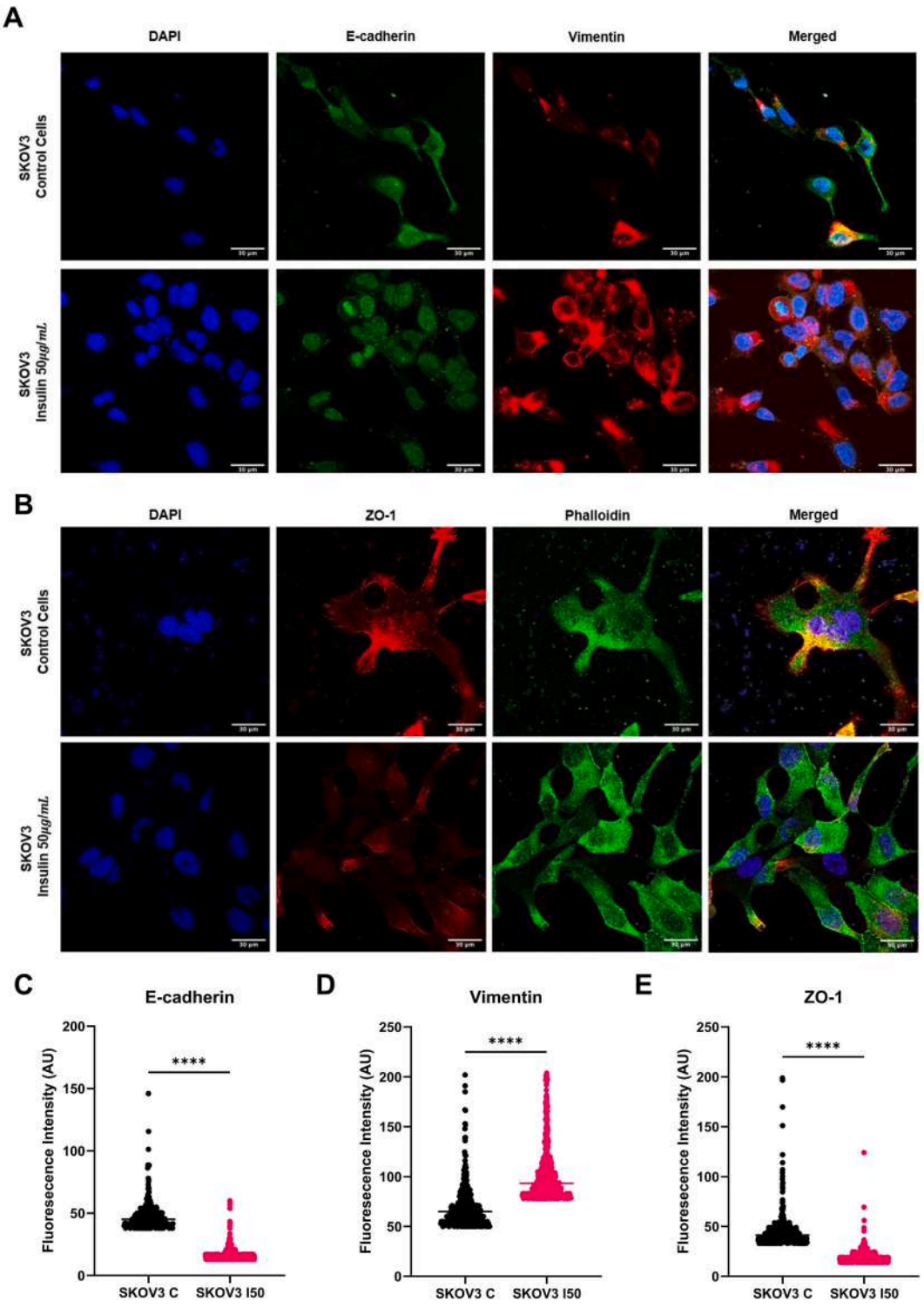

Fig. 4. Chronic insulin exposure promotes EMT-like protein expression changes in SKOV3 cells. A. E-cadherin (green) and vimentin (red) levels in control (top row) and insulin-treated (bottom row) SKOV3 cells. Nuclear DNA was stained with DAPI (blue). Qualitatively, E-cadherin levels decreased, while vimentin levels increased in cells grown under insulin compared to untreated cells. **B.** ZO-1 (red) and phalloidin (green) levels in control (top row) and insulin-treated (bottom row) SKOV3 cells. Nuclear DNA was stained with DAPI (blue). Qualitatively, ZO-1 levels decreased in cells grown under insulin compared to untreated cells. **C-E.** E-cadherin, vimentin and ZO-1 pixel intensity analysis confirms the downregulation of E-cadherin and ZO-1 expression, and the upregulation of vimentin expression, in cells treated with insulin. *C* denotes control samples, while *I50* represents cells cultured with 50 μg/mL insulin. Control and insulin-treated SKOV3 cells were cultured for 28 days in the media described in Section 2.6 of Methods. Statistical significance was determined using the threshold $P \leq .0001$ (****). All fluorescence images were acquired at the threshold limit of emission to avoid signal saturation.

establish whether MMP-9 upregulation is a direct consequence of TGF-beta upregulation or whether both changes represent parallel responses to insulin exposure. Therefore, these findings are interpreted as associated transcriptional changes rather than evidence of a defined TGF-beta-to-MMP-9 regulatory mechanism.

The observed temporal pattern is compatible with activation of insulin-responsive signalling pathways during prolonged insulin exposure. Western blot analysis showed time- and concentration-dependent changes in AKT and ERK phosphorylation, and p-IRS immunofluorescence was increased in insulin-treated cells (Fig. 3A and C). These findings support an association between insulin exposure and activation of signalling markers linked to migration, proliferation, and differentiation. However, because no pathway inhibition or receptor-specific validation was performed, the data do not establish a causal sequence linking TGF-beta, AKT/ERK activation, MMP-9 expression, and the functional invasion phenotype.

SMAD3 expression was elevated at earlier time points and lower insulin concentrations, potentially reflecting early activation of canonical TGF-β signalling prior to engagement of non-canonical pathways such as PI3K/AKT and MAPK/ERK [41]. SMAD-dependent signalling as an initial mediator of EMT transcriptional reprogramming [29], followed by non-canonical pathway activation that reinforces phenotypic plasticity and invasive behavior [30].

Both TGF-beta and MMP-9 were upregulated after insulin treatment (Fig. 2), and MMP-9 is associated with extracellular matrix remodelling and invasion. These transcriptional changes coincided with increased migration and invasion *in vitro* (Fig. 3B), particularly at higher insulin concentrations. However, the present study does not establish a direct causal relationship between TGF-beta upregulation, MMP-9 expression, and the functional phenotype. The findings are therefore interpreted as correlative EMT-associated and invasion-associated changes after chronic insulin exposure. This interpretation is supported by decreased E-cadherin and ZO-1 expression and increased vimentin expression (Fig. 4), consistent with an EMT-like phenotype.

Nevertheless, while MMP-9 expression increased significantly with higher insulin doses, the migratory and invasive capacities plateaued, suggesting that post-translational modifications might limit MMP-9 activity. This aligns with the understanding that MMPs are secreted as inactive proenzymes, that require proteolytic activation [42].

Several limitations should be considered when interpreting these findings. First, migration and invasion assays, together with EMT-associated marker expression, are *in vitro* surrogate endpoints and do not directly demonstrate metastatic dissemination. Second, although p-IRS, p-AKT, and p-ERK analyzes indicate changes in insulin-responsive signalling markers, pathway inhibition and receptor-specific validation were not performed; therefore, mechanistic conclusions remain correlative. Third, EMT characterization was based on RT-qPCR, quantitative immunocytochemistry, and functional assays, but did not include Western blot validation of EMT markers or assessment of EMT transcription factors. Finally, the main functional, signalling, and protein-level experiments were performed in SKOV3 cells, while A549 and MDA-MB-231 analyzes were limited to selected RT-qPCR markers. Additional ovarian cancer models and *in vivo* studies will be required to determine the generalizability and physiological relevance of these observations.

In conclusion, chronic insulin exposure was associated with EMT-like transcriptional and protein marker changes, activation of insulin-responsive signalling markers, and increased migration and invasion in SKOV3 ovarian cancer cells *in vitro*. The temporal sequence observed—early SMAD3 activation, followed by AKT/ERK signalling and subsequent MMP-9 upregulation—supports a model in which insulin may promote cellular traits relevant to invasion and metastatic progression; however, the present study does not directly demonstrate metastatic dissemination or define a causal signalling sequence. These results support growing evidence that metabolic disorders, including insulin resistance, obesity, and type 2 diabetes mellitus, are associated with increased cancer risk and poorer metastatic outcomes following primary tumor diagnosis. Beyond its canonical role in metabolic regulation, insulin may contribute to tumor progression by influencing cellular plasticity and modulating the TME, thereby facilitating pro-metastatic cellular changes. These observations highlight the need to further investigate how metabolic and hormonal signalling pathways influence tumor cell plasticity, but additional studies using pathway inhibition, receptor-specific validation, EMT transcription factor analysis, quantitative protein validation, additional ovarian cancer models, and *in vivo* metastasis models will be required to determine physiological relevance.

CRediT authorship contribution statement

Jaume Margalef Rieres: Writing – review & editing, Writing – original draft, Methodology, Formal analysis, Data curation, Conceptualization. **Patricia González-Sáenz:** Writing – review & editing, Methodology, Formal analysis, Data curation. **Sylvain Ladame:** Writing – review & editing, Writing – original draft, Supervision, Project administration, Funding acquisition, Conceptualization. **Nuria Oliva:** Writing – review & editing, Writing – original draft, Supervision, Resources, Project administration, Methodology, Funding acquisition, Conceptualization.

Declaration of competing interest

The authors declare the following financial interests/personal relationships which may be considered as potential competing interests: Nuria Oliva reports financial support was provided by LaCaixa Foundation (LCF/BQ/PR22/11920009). If there are other authors, they declare that they have no known competing financial interests or personal relationships that could have appeared to influence the work reported in this paper.

Acknowledgements

We thank Dr. Claire Higgins for providing the primary antibodies for immunostaining experiments, Dr. Jose Antonio Duran-Mota for assistance with the confocal fluorescence microscope and Dr. Oliver Teenan for advice on qPCR data analysis. We also thank Dr. Michael Bruyns-Haylett for advice writing the manuscript. NO acknowledges a la Caixa Foundation Junior Leader Fellowship (LCF/BQ/PR22/11920009).

Appendix A. Supplementary data

Supplementary data to this article can be found online at https://doi.org/10.1016/j.adcanc.2026.100184.

Data availability

Data will be made available on request.

References

[1] K. Mani, et al., Causes of death among people living with metastatic cancer, Nat. Commun. 15 (2024).
[2] H. Sung, et al., Global patterns in excess body weight and the associated cancer burden, CA Cancer J. Clin. 69 (2019) 88–112.
[3] X. Hu, et al., Type 2 diabetes mellitus promotes the proliferation, metastasis, and suppresses the apoptosis in oral squamous cell carcinoma, J. Oral Pathol. Med. 51 (2022) 483–492.
[4] E. Giovannucci, et al., Diabetes and cancer: a consensus report, Diabetes Care 33 (2010) 1674–1685.
[5] M.M. Baleiras, et al., Prognostic impact of type 2 diabetes in metastatic colorectal cancer, Cureus (2023), https://doi.org/10.7759/cureus.33916, 10.7759/cureus.33916.
[6] L. Hutchinson, Understanding metastasis, Nat. Rev. Clin. Oncol. 12 (2015), 247–247.

[7] C. Biray Avci, et al., Tumor microenvironment and cancer metastasis: molecular mechanisms and therapeutic implications, Front. Pharmacol. 15 (2024).
[8] M.I. Diaz Bessone, M.J. Gattas, T. Laporte, M. Tanaka, M. Simian, The Tumor microenvironment as a Regulator of endocrine resistance in breast cancer, Front. Endocrinol. 10 (2019).
[9] S. Xie, J. Pan, J. Xu, W. Zhu, L. Qin, The critical function of metabolic reprogramming in cancer metastasis, Aging Cancer 3 (2022) 20–43.
[10] P. Gui, T.G. Bivona, Evolution of metastasis: new tools and insights, Trends Cancer 8 (2022) 98–109.
[11] P.S. Steeg, Tumor metastasis: mechanistic insights and clinical challenges, Nat. Med. 12 (2006) 895–904.
[12] T. Liu, L. Zhang, D. Joo, S.-C. Sun, NF-κB signaling in inflammation, Signal Transduct. Targeted Ther. 2 (2017) 17023.
[13] M. Owyong, et al., MMP9 modulates the metastatic cascade and immune landscape for breast cancer anti-metastatic therapy, Life Sci. Alliance 2 (2019) e201800226.
[14] E. Batlle, et al., The transcription factor Snail is a repressor of E-cadherin gene expression in epithelial tumour cells, Nat. Cell Biol. 2 (2000) 84–89.
[15] S. Valastyan, R.A. Weinberg, Tumor metastasis: molecular insights and evolving paradigms, Cell 147 (2011) 275–292.
[16] O.G. McDonald, H. Wu, W. Timp, A. Doi, A.P. Feinberg, Genome-scale epigenetic reprogramming during epithelial-to-mesenchymal transition, Nat. Struct. Mol. Biol. 18 (2011) 867–874.
[17] R.A. Haeusler, T.E. McGraw, D. Accili, Biochemical and cellular properties of insulin receptor signalling, Nat. Rev. Mol. Cell Biol. 19 (2018) 31–44.
[18] K. Staiger, A. Hennige, H. Staiger, H.-U. Häring, M. Kellerer, Comparison of the mitogenic potency of regular human insulin and its analogue glargine in normal and transformed human breast epithelial cells, Horm. Metab. Res. 39 (2007) 65–67.
[19] L. Makowski, S. Sundaram, A. Johnson, Obesity, metabolism and the microenvironment: links to cancer, J. Carcinog. 12 (2013) 19.
[20] L. Li, et al., The Ras/Raf/MEK/ERK signaling pathway and its role in the occurrence and development of HCC, Oncol. Lett. 12 (2016) 3045–3050.
[21] Y. Wang, et al., Insulin promotes proliferation, survival, and invasion in endometrial carcinoma by activating the MEK/ERK pathway, Cancer Lett. 322 (2012) 223–231.
[22] B.P. Leitner, S. Siebel, N.D. Akingbesote, X. Zhang, R.J. Perry, Insulin and cancer: a tangled web, Biochem. J. 479 (2022) 583–607, https://doi.org/10.1042/BCJ20210134. Preprint at.
[23] R. Malaguarnera, A. Belfiore, The insulin receptor: a new target for cancer therapy, Front. Endocrinol. 2 (2011), https://doi.org/10.3389/fendo.2011.00093. Preprint at.
[24] T. Tsujimoto, H. Kajio, T. Sugiyama, Association between hyperinsulinemia and increased risk of cancer death in nonobese and obese people: a population-based observational study, Int. J. Cancer 141 (2017) 102–111.
[25] P.R. Bonagiri, J.H. Shubrook, Review of associations between type 2 diabetes and cancer. https://doi.org/10.2337/figshare.12149484, 2020.
[26] L. Szablewski, Insulin resistance: the increased risk of cancers, Curr. Oncol. 31 (2024) 998–1027, https://doi.org/10.3390/curroncol31020075. Preprint at.
[27] M. Janghorbani, M. Dehghani, M. Salehi-Marzijarani, Systematic review and meta-analysis of insulin therapy and risk of cancer, Hormones Cancer 3 (2012) 137–146, https://doi.org/10.1007/s12672-012-0112-z. Preprint at.
[28] D. Laskowski, et al., Insulin concentrations used in in vitro embryo production systems: a pilot study on insulin stability with an emphasis on concentrations measured in vivo, Acta Vet. Scand. 58 (2016) 66.
[29] M. Shin, E.G. Yang, H.K. Song, H. Jeon, Insulin activates EGFR by stimulating its interaction with IGF-1R in low-EGFR-expressing TNBC cells, BMB Rep. 48 (2015) 342–347.
[30] S. Krajnak, et al., The impact of insulin on low-dose metronomic vinorelbine and mafosfamide in breast cancer cells, Anticancer Res. 41 (2021) 1243–1250.
[31] M.V. Sefton, G.M. Antonacci, Adsorption isotherms of insulin onto various materials, Diabetes 33 (1984) 674–680.
[32] T.M. Keenan, A. Folch, Biomolecular gradients in cell culture systems, Lab Chip 8 (2008) 34–57.
[33] R. Dhumpa, M.G. Roper, Temporal gradients in microfluidic systems to probe cellular dynamics: a review, Anal. Chim. Acta 743 (2012) 9–18.
[34] T.-Y. Na, L. Schecterson, A.M. Mendonsa, B.M. Gumbiner, The Functional Activity of E-cadherin Controls Tumor Cell Metastasis at Multiple Steps, vol 117, Proceedings of the National Academy of Sciences, 2020, pp. 5931–5937.
[35] X. Zhang, et al., Decreased expression of ZO-1 is associated with tumor metastases in liver cancer, Oncol. Lett. (2018), https://doi.org/10.3892/ol.2018.9765, 10.3892/ol.2018.9765.
[36] S. Usman, et al., Vimentin is at the heart of Epithelial Mesenchymal Transition (EMT) mediated metastasis, Cancers (Basel) 13 (2021) 4985.
[37] I. Kareva, From hyperinsulinemia to cancer progression: how diminishing glucose storage capacity fuels insulin resistance, Aging Cancer 5 (2024) 51–61.
[38] T. Tsujimoto, H. Kajio, T. Sugiyama, Association between hyperinsulinemia and increased risk of cancer death in nonobese and obese people: a population-based observational study, Int. J. Cancer 141 (2017) 102–111.
[39] C.-C. Lu, et al., Insulin induction instigates cell proliferation and metastasis in human colorectal cancer cells, Int. J. Oncol. 50 (2017) 736–744.
[40] B. Bierie, H.L. Moses, TGFβ: the molecular Jekyll and Hyde of cancer, Nat. Rev. Cancer 6 (2006) 506–520.
[41] M. Davies, et al., Induction of an epithelial to mesenchymal transition in human immortal and malignant keratinocytes by TGF-β1 involves MAPK, Smad and AP-1 signalling pathways, J. Cell. Biochem. 95 (2005) 918–931.
[42] M. Quiding-Jarbrink, D.A. Smith, G.J. Bancroft, Production of matrix metalloproteinases in response to mycobacterial infection, Infect. Immun. 69 (2001) 5661–5670.